Collaborative Research Center CRC 110

"Symmetries and the emergence of structure in QCD"

Two CRC periods of project B.11 (FP 2 and 3)

"Coupled-channel dynamics"

CRC 110 Final Meeting, Bonn, June 2024

| PL's: Bing-Song Zou , Deborah Rönchen

In collaboration with: M. Döring, J. Hergenrather, M. Mai, T. Mart, Ulf-G. Meißner, S. Rawat, C. Schneider, C.-W. Shen, Y.-F. Wang, Z.-L. Wang, R. Workman |

The excited baryon spectrum:

Connection between experiment and QCD in the non-perturbative regime

Experimental study of hadronic reactions

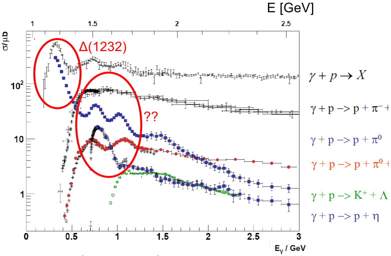

source: ELSA; data: ELSA, JLab, MAMI

⟺

Theoretical predictions of excited hadrons
e.g. from relativistic quark models:

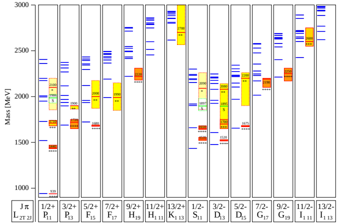

Löring *et al.* EPJ A 10, 395 (2001), experimental spectrum: PDG 2000

Goals:

- Extraction of N^*, Δ^* **and** Y^* **resonances** in pion-, kaon-, photon- and electron induced reactions using a **dynamical coupled-channel** (DCC) approach
- Analysis of states in the hidden-charm (-beauty) sector, P_c states

Methods:

- Jülich-Bonn dynamical coupled-channels model ("JüBo DCC")

JÜLICH Forschungszentrum

The Jülich-Bonn DCC approach for N^* and Δ^*

EPJ A 49, 44 (2013)

Dynamical coupled-channels (DCC): **simultaneous** analysis of different reactions

The scattering equation in partial-wave basis

$$\langle L'S'p'|T^{IJ}_{\mu\nu}|LSp\rangle = \langle L'S'p'|V^{IJ}_{\mu\nu}|LSp\rangle + \sum_{\gamma,L''S''}\int_0^\infty dq \quad q^2 \quad \langle L'S'p'|V^{IJ}_{\mu\gamma}|L''S''q\rangle \frac{1}{E - E_\gamma(q) + i\epsilon}\langle L''S''q|T^{IJ}_{\gamma\nu}|LSp\rangle$$

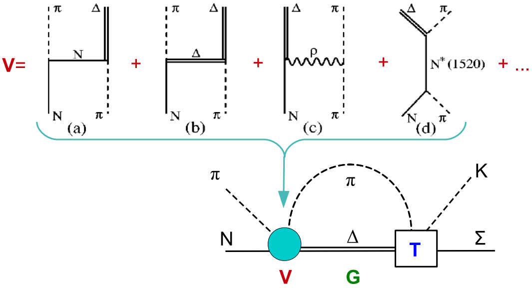

- theoretical constraints on the $\mathcal{S}$ matrix: **unitarity** and **analyticity**
- resonances = poles on the 2nd Riemann sheet of T
- hadronic reactions: potentials V constructed from effective $\mathcal{L}$
- s-channel diagrams: T^P
  genuine resonance states
- t- and u-channel: T^{NP}
  (dynamical generation of poles)

The Jülich-Bonn DCC approach for N^* and Δ^*

EPJ A 49, 44 (2013)

Dynamical coupled-channels (DCC): **simultaneous** analysis of different reactions

The scattering equation in partial-wave basis

$$\langle L'S'p'|T^{IJ}_{\mu\nu}|LSp\rangle = \langle L'S'p'|V^{IJ}_{\mu\nu}|LSp\rangle + \sum_{\gamma,L''S''}\int_0^\infty dq \quad q^2 \quad \langle L'S'p'|V^{IJ}_{\mu\gamma}|L''S''q\rangle \frac{1}{E-E_\gamma(q)+i\epsilon}\langle L''S''q|T^{IJ}_{\gamma\nu}|LSp\rangle$$

- hadronic channels ν, μ, γ:

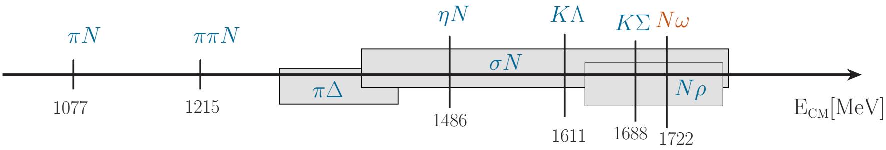

The Jülich-Bonn DCC approach for N^* and Δ^*

EPJ A 49, 44 (2013)

Dynamical coupled-channels (DCC): **simultaneous** analysis of different reactions

The scattering equation in partial-wave basis

$$\langle L'S'p'|T^{IJ}_{\mu\nu}|LSp\rangle = \langle L'S'p'|V^{IJ}_{\mu\nu}|LSp\rangle + \sum_{\gamma,L''S''}\int_0^\infty dq \quad q^2 \quad \langle L'S'p'|V^{IJ}_{\mu\gamma}|L''S''q\rangle \frac{1}{E-E_\gamma(q)+i\epsilon} \langle L''S''q|T^{IJ}_{\gamma\nu}|LSp\rangle$$

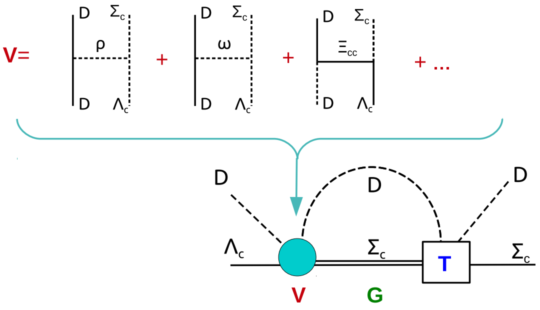

- theoretical constraints on the $\mathcal{S}$ matrix: **unitarity** and **analyticity**
- resonances = poles on the 2nd Riemann sheet of T
- hadronic reactions: potentials V constructed from effective $\mathcal{L}$
- s-channel diagrams: T^P genuine resonance states
- t- and u-channel: T^{NP} (dynamical generation of poles)

The Jülich-Bonn DCC approach for N^* and Δ^*

EPJ A 49, 44 (2013)

Dynamical coupled-channels (DCC): **simultaneous** analysis of different reactions

The scattering equation in partial-wave basis

$$\langle L'S'p'|T^{IJ}_{\mu\nu}|LSp\rangle = \langle L'S'p'|V^{IJ}_{\mu\nu}|LSp\rangle + \sum_{\gamma,L''S''}\int_0^\infty dq \quad q^2 \quad \langle L'S'p'|V^{IJ}_{\mu\gamma}|L''S''q\rangle \frac{1}{E-E_\gamma(q)+i\epsilon}\langle L''S''q|T^{IJ}_{\gamma\nu}|LSp\rangle$$

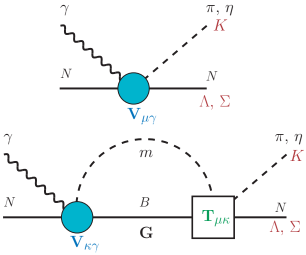

- theoretical constraints on the $\mathcal{S}$ matrix: **unitarity** and **analyticity**
- resonances = poles on the 2nd Riemann sheet of T
- photon/electron reactions: potentials V energy-dependent polynomials
- $T_{\mu\kappa}$: full hadronic T-matrix $\rightarrow$ simultaneous fit of pion- and photon (electron) induced reactions

Progress during the CRC 110 FPs 2 and 3

- Inclusion of the $\pi N \to \omega N$ channel (Yu-Fei Wang *et al.* PRD 106 (2022))
  (ωN channel not yet included in photoproduction fits)

Extension of the JüBo model to $K\Lambda$ photoproduction on the proton (EPJA 54 (2018) 110):

- Simultaneous analysis of $\pi N \to \pi N, \eta N, K\Lambda, K\Sigma$ and
  $\gamma p \to \pi N, \eta N, K\Lambda$
- determination of the N^* and Δ^* states, e.g. confirmation of the $N(1900)3/2^+$

Λ decay parameter α_-:

- BESIII measurement ($e^+e^- \to J/\psi \to \Lambda\bar{\Lambda}$):
  $\alpha_- = 0.750 \pm 0.009 \pm 0.004$ (Ablikim, Nature (2019))
- independent estimation from $\gamma p \to K^+\Lambda$ CLAS data using Fierz identities
  $\Rightarrow \alpha_- = 0.721 \pm 0.006 \pm 0.005$ (Ireland et al. PRL 123 (2019)) (PDG average until 2019: $\alpha_- = 0.642 \pm 0.013$)

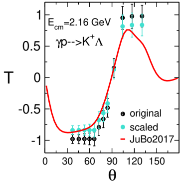

data: Paterson (CLAS) PRC 93, 065201 (2016)

- Analysis of new CLAS eta photoproduction data, P. Collins *et al.* PLB 771, 213 (2017)

Extension to $K\Sigma$ photoproduction on the proton

JüBo2022 Eur.Phys.J.A 58 (2022) 229

Simultaneous analysis of $\pi N \to \pi N, \eta N, K\Lambda, K\Sigma$ and $\gamma p \to \pi N, \eta N, K\Lambda, K\Sigma$

- almost 72,000 data points in total, $W_{\text{max}} = 2.4$ GeV
  - $\gamma p \to K^+\Sigma^0$: $d\sigma/d\Omega$, P, Σ, T, $C_{x',z'}$, $O_{x,z}$ = 5,652
  - $\gamma p \to K^0\Sigma^+$: $d\sigma/d\Omega$, P = 448
- polarizations scaled by new Λ decay constant α_- (Ireland PRL 123 (2019), 182301), if applicable
- χ^2 minimization with MINUIT on JURECA [Jülich Supercomputing Centre, JURECA: JLSRF 2, A62 (2016)]

Resonance analysis:

- all PDG 4-star N and Δ states up to $J = 9/2$ are seen (exception: $N(1895)1/2^-$) + some states rated less than 4 stars
- no additional s-channel diagram, but indications for new dyn. gen. poles

New data on $\gamma p \to K^0\Sigma^+$ by CLAS L. Clark et al. 2404.19404
more (double) polarization observables → JüBo2023-1 fit

Selected fit results

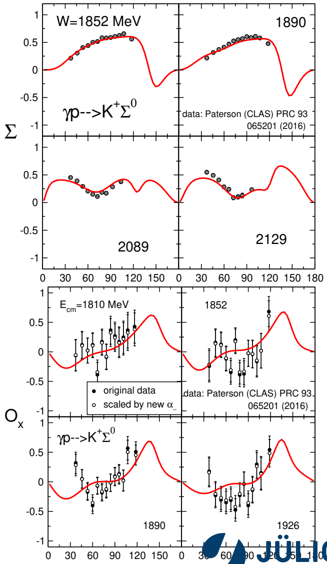

On the nature of N^* and Δ states

Y.-F. Wang et al. PRC 109 (2024)

Elementary or composite state?

Weinberg's criterion (deuteron) for elementariness Z

- from scattering length a and effective range r :

$$a = -\frac{2(1-Z)}{2-Z}R + \mathcal{O}(L) \qquad r = -\frac{Z}{1-Z}R + \mathcal{O}(L)\,;$$

  $R = (2\mu B)^{-1/2} \simeq 4.3$ fm deuteron radius, $L = 1/M_\pi \simeq 1.4$ fm interaction range,

- experiment: $a = -5.41$ fm , $r = 1.75$ fm $\rightarrow$ small Z $\rightarrow$ deuteron composed of two nucleons
- conditions: S-wave, near-threshold, stable

Modern generalizations:

- Higher partial waves, broad resonances, not close to thresholds
- among other approaches: spectral density functions [Baru et al., PLB 586, 53 (2004)]
- apply to comprehensive data driven models $\rightarrow$ meaningful results

On the nature of N^* and Δ states

Y.-F. Wang et al. PRC 109 (2024)

Coupled-channel formalisim

- coupled channels: elementariness Z disperses into a finite probability distribution $w(z) \sim$ "spectral density function"
- mathematically: $w(z)$ projection of physical scattering state (with energy z) on bare elementary state

$w_i(z) = -\frac{1}{\pi}\text{Im}D_{ii}(z)$ $\quad D_{ii}$ dressed propagator of bare s-channel state i, includes full coupled-channel T matrix

$$\mathcal{Z}_i \simeq \frac{\int_{M_R-\Gamma_R}^{M_R+\Gamma_R} w_i(z)dz}{\int_{M_R-\Gamma_R}^{M_R+\Gamma_R} BW(z)dz}\,, \qquad BW(z) \equiv \frac{1}{\pi}\frac{\Gamma_R/2}{(z-E_R)^2+(\Gamma_R/2)^2}$$

- more than one bare state in a PW: Total elementariness:

$$\mathcal{Z} = 1 - \prod_i (1-\mathcal{Z}_i)$$

On the nature of N^* and Δ states

Y.-F. Wang et al. PRC 109 (2024)

Application to the JüBo2022 resonances

Selected results for N^* states: spectral density functions

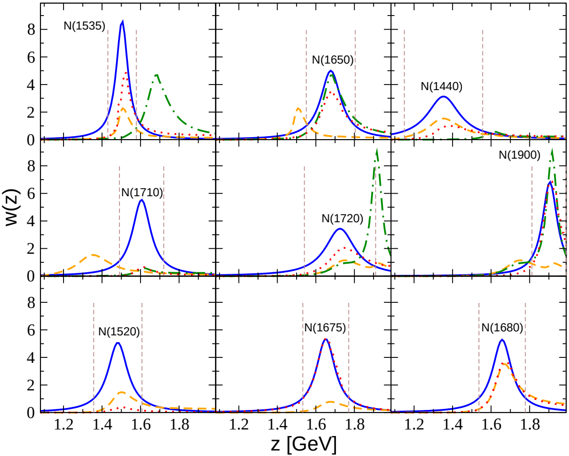

Blue solid line: BW denominator

Orange dashed (green dash-dotted): 1st (2nd) spectral density function (model)

Red dotted: locally constructed function

Vertical lines: the integral region

On the nature of N^* and Δ states

Y.-F. Wang et al. PRC 109 (2024)

Application to the JüBo2022 resonances

Selected results for N^* states: elementariness

State	Pole position (MeV)	$\mathcal{Z}_1$	$\mathcal{Z}_2$	$\mathcal{Z}_{\text{tot}}$	$\mathcal{Z}^{\text{lc}}$
$N(1535)\ \frac{1}{2}^-$	$1504-37i$	24.8%	5.6%	29.0%	50.8%
$N(1650)\ \frac{1}{2}^-$	$1678-64i$	13.4%	91.7%	92.8%	70.5%
$N(1440)\ \frac{1}{2}^+$	$1353-102i$	48.7%	1.7%	49.5%	31.5%
$N(1710)\ \frac{1}{2}^+$	$1605-58i$	11.5%	10.3%	20.6%	10.2%
$N(1720)\ \frac{3}{2}^+$	$1726-93i$	34.1%	68.5%	79.3%	62.5%
$N(1900)\ \frac{3}{2}^+$	$1905-47i$	19.9%	100%	100%	99.9%
$N(1520)\ \frac{3}{2}^-$	$1482-63i$	29.4%	$\cdots$	29.4%	7.2%
$N(1680)\ \frac{5}{2}^+$	$1657-60i$	67.9%	$\cdots$	67.9%	69.9%

Green: high compositeness, blue: high elementariness

Electroproduction

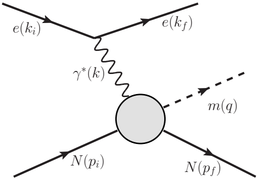

Experimental studies of electroproduction:

major progress in recent years, e.g., from JLab, MAMI, ...

- 10^5 data points for πN, ηN, KY, $\pi\pi N$ electroproduction
- access the Q^2 dependence of the amplitude

  $\rightarrow$ expected to provide a link between perturbative QCD and the region where quark confinement sets in

- so far, no new N^* or Δ^* established from electroproduction: data not yet analyzed on the same level as photoproduction
  Reviews: Prog.Part.Nucl.Phys. 67 (2012); Few. Body Syst. 63 (2022) 3, 59

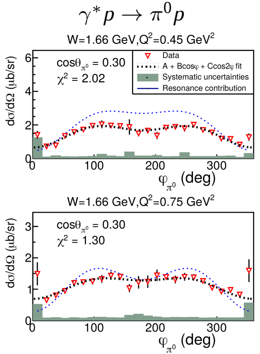

Figure and data from Markov et al. (CLAS) PRC 101 (2020), resonance contribution: JLab/YerPhI

Single-channels analyses, e.g.:

- MAID: π, η, kaon electroproduction (EPJA 34, 69 (2007), NPA 700, 429 (2002),)
- JLab: π electroproduction covering the resonance region (PRC 80 (2009) 055203)

Coupled-channels analyses:

- ANL-Osaka: extension of DCC analysis of pion electroproduction (PRC 80, 025207 (2009)) in progress (Few Body Syst. 59 (2018) 3, 24)
- Jülich-Bonn-Washington approach M. Mai *et al.* PRC 103 (2021): $\gamma^* p \rightarrow \pi^0 p$, $\pi^+ n$, ηp, $K\Lambda$

JÜLICH Forschungszentrum

Jülich-Bonn-Washington (JBW) parametrization

M. Mai *et al.* PRC 103 (2021), PRC 106 (2022), EPJ A 59 (2023)

$$\mathcal{M}_{\mu\gamma^*}(k,W,Q^2) = R_{\ell'}(\lambda, q/q_\gamma)\left(V_{\mu\gamma^*}(k,W,Q^2) + \sum_\kappa \int_0^\infty dp\, p^2\, T_{\mu\kappa}(k,p,W) G_\kappa(p,W) V_{\kappa\gamma^*}(p,W,Q^2)\right)$$

(Pseudo)-threshold behavior with meson/photon momenta

$$lim_{k\to 0} E_{\ell+} = k^\ell$$
$$lim_{q\to 0} L_{\ell+} = q^\ell$$
$$\dots$$

For $Q^2=0$ (real photons) identical to Jülich-Bonn photoproduction amplitude

$$V_{\mu\gamma^*}(k,W,Q^2) = V^{\text{JUBO}}_{\mu\gamma}(k,W)\cdot \tilde{F}_D(Q^2)\cdot e^{-\beta^0_\mu Q^2/m_p^2}\left(1 + Q^2/m_p^2\beta^1_\mu + (Q^2/m_p^2)^2\beta^2_\mu\right)$$

$\leftarrow$ Siegerts's theorem Siegert(1973) Amaldi et al.(1979) Tiator(2016)

$$V^{L_{\ell\pm}} = (\text{const.})\cdot V^{E_{\ell\pm}}$$

...at pseudo-threshold

- simultaneous fit to πN, ηN, $K\Lambda$ electroproduction off proton ($W < 1.8$ GeV, $Q^2 < 8$ GeV^2)
- 533 fit parameters, 110.281 data points
- Input from JüBo: $V_{\mu\gamma}(k,W,Q^2=0)$, $T_{\mu\kappa}(k,p,W)$, $G_\kappa(p,W)$

  $\rightarrow$ universal pole positions and residues (fixed in this study)
- long-term goal: fit pion-, photo- and electron-induced reactions simultaneously

$\gamma^* p \rightarrow K\Lambda$ at $W = 1.7$ GeV

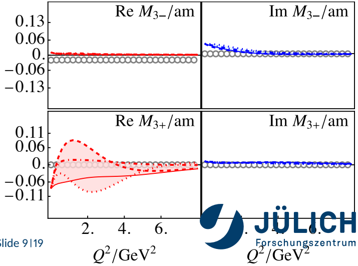

Baryon Transition Form Factors

Y.-F. Wang et al. 2404.17444 [nucl-th]

based on most recent JBW, JüBo2022

Q^2 dependence of transition form factors (TFFs) allows conclusions on the nature of resonances.

Here:

- for the first time determined from a coupled-channel study of πN, ηN, and $K\Lambda$ electroproduction (+ constraints from photon and pion-induced reactions)
- first estimation of TFFs for higher excited states
- from poles, not Breit-Wigner states

TFFs defined independently of the hadronic final state as Workman et al. PRC 87 (2013) :

$$H_h^{l\pm,I}(Q^2) = C_I \sqrt{\frac{p_{\pi N}}{\omega_0} \frac{2\pi(2J+1)z_p}{m_N \widetilde{R}^{l\pm,I}}} \widetilde{\mathcal{H}}_h^{l\pm,I}(Q^2)\,,$$

$h = 1/2, 3/2$ helicity, $\mathcal{H}$ ($=\mathcal{A}$ or $\mathcal{S}$) helicity amplitudes, $\widetilde{\mathcal{H}}$, $\widetilde{R}$ residues, z_p pole position

Baryon Transition Form Factors

Y.-F. Wang et al. 2404.17444 [nucl-th]

based on most recent JBW, JüBo2022

Δ states:

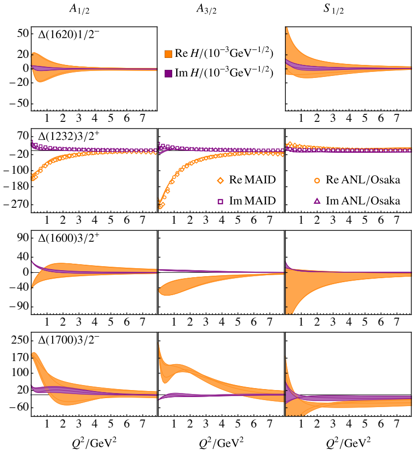

[ANL/OSAKA: Kamano Few Body Syst. 59, 24 (2018), MAID: Tiator et al. PRC94 (2016)]

Baryon Transition Form Factors

Y.-F. Wang et al. 2404.17444 [nucl-th]

based on most recent JBW, JüBo2022

N^* states:

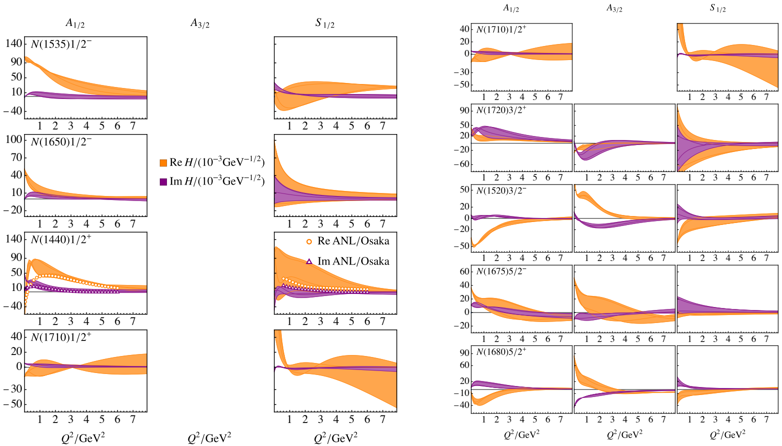

[ANL/OSAKA: Kamano Few Body Syst. 59, 24 (2018), MAID: Tiator et al. PRC94 (2016)]

Baryon Transition Form Factors

Y.-F. Wang et al. 2404.17444 [nucl-th]

based on most recent JBW, JüBo2022

The Roper resonance $N(1440)1/2^+$:

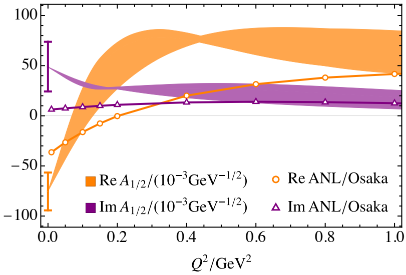

- Zero crossing in Re$A_{1/2}$ at smaller Q^2 than in Breit-Wigner determinations or in ANL/OSAKA
  [Kamano, Few Body Syst. 59, 24 (2018)]
- important for quark models, DSE: meson cloud contributions or radial excitation of the nucleon?

Transverse charge density ρ of $p \to N(1440)$ transition:

following Tiator et al. Chin. Phys. C 33 (2009)

- study flavor decomposition, u and d quark distribution

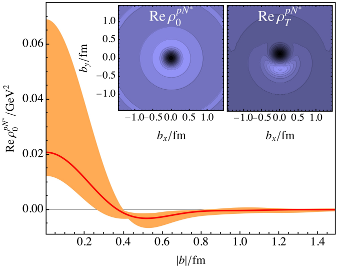

Orange band: JBW, red line: MAID 2007.
Insets: light/dark shades represent negative/positive values
b: transverse position in xy-plane

Hidden charm reactions

Hidden charm reactions in JüBo Wang, Shen, Rönchen, Meißner, Zou

$\bar{D}^{(*)}\Lambda_c - \bar{D}^{(*)}\Sigma_c^{(*)}$ interactions

EPJ C 82, 497 (2022)

- 2017: exploratory study of only two channels, $\bar{D}\Lambda_c$ and $\bar{D}\Sigma_c$ Shen *et al.* CPC 42, 023106 (2018)
- 2022: extension to a more complete coupled-channel calculation: $\bar{D}\Lambda_c$, $\bar{D}\Sigma_c$, $\bar{D}^*\Lambda_c$, $\bar{D}^*\Sigma_c$, $\bar{D}\Sigma_c^*$
  $\rightarrow$ more comprehensive picture of the hidden-charm resonance spectrum
  $\rightarrow$ postdict LHCb pentaquarks by tuning free parameters, predict additional dyn. gen. states

Selected results:

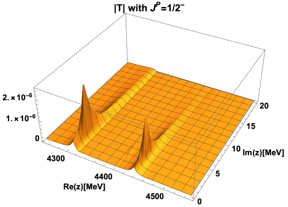

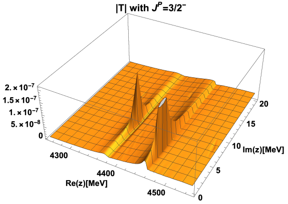

$J^P = 1/2^-$, $I = 1/2$:

- $z_0 = 4312.4 - i2.9$ MeV ($\bar{D}\Sigma_c$ bound state) $\rightarrow$ LHCb $P_c(4312)$ Aaij *et al.* PRL 122, 222001 (2019)
- $z_0 = 4439.4 - i2.8$ MeV ($\bar{D}^*\Sigma_c$ bound state) $\rightarrow$ LHCb $P_c(4440)$ Aaij *et al.* PRL 122, 222001 (2019)

$J^P = 3/2^-$, $I = 1/2$:

- $z_0 = 4375.9 - i7.6$ MeV ($\bar{D}\Sigma_c^*$ bound state)
- $z_0 = 4460.0 - i3.9$ MeV ($\bar{D}^*\Sigma_c$ bound state) $\rightarrow$ LHCb $P_c(4457)$ Aaij *et al.* PRL 122, 222001 (2019)

$J^P = 1/2^+$, $I = 1/2$:

- $z_0 = 4339.3 - i106.3$ MeV $\rightarrow$ LHCb $P_c(4337)$? Aaij *et al.* PRL 128, 062001 (2022)

+ several resonances in higher PWs

P_c states from fit to LHCb data

C.-W Shen et al. 2405.02626 [hep-ph]

$J/\psi p$ invariant mass distributions in the $\Lambda_b^0 \to J/\psi p K^-$ decay

→ extend framework to $J/\psi N$ channel

- $J/\psi p$ invariant mass distribution:

$$\frac{d\Gamma}{dm_{J/\psi p}} = \frac{\tilde{q}_{J/\psi} q_K}{4(2\pi)^3 m_{\Lambda_b}} \left(\sum_{J=1/2}^{5/2} |T^J|^2 + |T_{bg}|^2 \right)$$

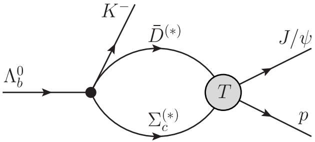

with

$$T^{1/2} = \sum_\kappa g_\kappa^{1/2}\ G_\kappa\ T^{1/2}_{\kappa\, J/\psi p}$$

$$T^{3/2} = \sum_\kappa g_\kappa^{3/2}\ G_\kappa\ T^{3/2}_{\kappa\, J/\psi p}\ q_K$$

$$T^{5/2} = \sum_\kappa g_\kappa^{5/2}\ G_\kappa\ T^{5/2}_{\kappa\, J/\psi p}\ q_K^2$$

g_κ^J: free fit parameters

$T^J_{\kappa\, J/\psi p}$, G_κ: coupled-channel T-matrix and propagator

Polynomial background term:

$$T_{bg} = a + bs + cs^2$$

s: Mandelstam variable; a, b, c: free fit parameters

P_c states from fit to LHCb data

C.-W Shen et al. 2405.02626 [hep-ph]

Three fit results with different starting values

Fit parameters:

- g^J_κ in T^J
- cut-offs in form factors of coupled-channel T-matrix
- a, b, c: free fit parameters in T_{bg}

$\rightarrow$ 33 fit parameters, 175 data points

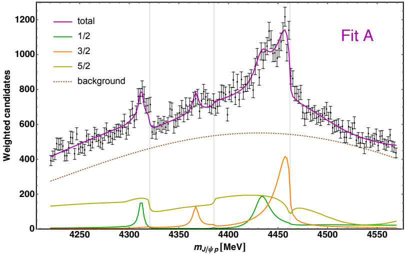

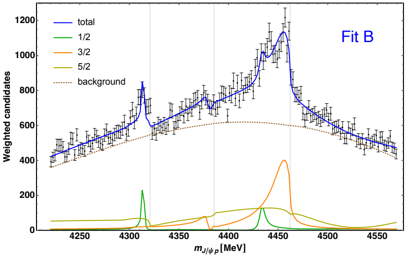

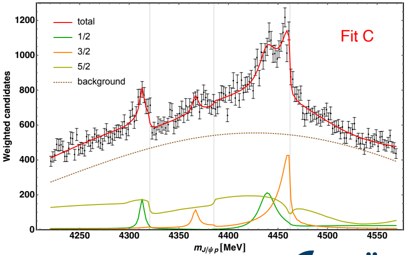

Data: R. Aaij et al. [LHCb], Phys. Rev. Lett. 122, 222001 (2019).

P_c states from fit to LHCb data

C.-W Shen et al. 2405.02626 [hep-ph]

Resonance analysis: 4 prominent narrow states

Fit	z_R , J^P
A	$4312.3 - i2.4,\ \frac{1}{2}^-$
B	$4314.0 - i0.74,\ \frac{1}{2}^-$
C	$4312.9 - i2.6,\ \frac{1}{2}^-$
A	$4366.5 - i4.7,\ \frac{3}{2}^-$
B	$4378.7 - i4.1,\ \frac{3}{2}^-$
C	$4365.9 - i4.7,\ \frac{3}{2}^-$
A	$4433.0 - i9.3,\ \frac{1}{2}^-$
B	$4433.4 - i3.2,\ \frac{1}{2}^-$
C	$4438.6 - i10,\ \frac{1}{2}^-$
A	$4461.4 - i9.7,\ \frac{3}{2}^-$
B	$4461.5 - i14,\ \frac{3}{2}^-$
C	$4464.9 - i6.8,\ \frac{3}{2}^-$

- just below $\bar{D}\Sigma_c$, strong coupling to $\bar{D}\Sigma_c$
  $\rightarrow \bar{D}\Sigma_c$ boundstate
- $P_c(4312)$

- $\bar{D}\Sigma_c^*$ bound state

- strong coupling to $\bar{D}^*\Sigma_c$, below $\bar{D}^*\Sigma_c$ threshold
  $\rightarrow$ likely a $\bar{D}^*\Sigma_c$ bound state
- $P_c(4440)$

- strong coupling to $\bar{D}^*\Sigma_c$
- below $\bar{D}^*\Sigma_c$ threshold in Fit A, B, above in Fit C
- $P_c(4457)$

P_c states from fit to LHCb data

C.-W Shen et al. 2405.02626 [hep-ph]

Resonance analysis: poles in higher partial waves

J^P	z_R [MeV]			
	Fit A	Fit B	Fit C	
$\frac{1}{2}^-$	$4408.1 - i181.5$	$4413.8 - i182.4$	$4407.1 - i178.1$	
$\frac{1}{2}^-$	$4475.7 - i143.6$	$4502.5 - i140.7$	$4476.4 - i143.9$	
$\frac{1}{2}^+$	$4337.2 - i76.3$	$4325.4 - i85.4$	$4335.1 - i75.3$	$P_c(4337)$?
$\frac{3}{2}^+$	$4413.0 - i197.0$	$4410.9 - i193.0$	$4413.3 - i196.0$	
$\frac{3}{2}^+$	$4387.9 - i156.3$	-	$4387.4 - i156.1$	$P_c(4380)$?
$\frac{3}{2}^-$	$4408.0 - i168.9$	$4408.3 - i175.9$	$4407.0 - i167.6$	
$\frac{3}{2}^-$	$4506.6 - i136.2$	$4501.5 - i132.3$	$4506.5 - i133.9$	
$\frac{5}{2}^-$	$4411.6 - i180.1$	-	$4411.6 - i179.9$	
$\frac{5}{2}^+$	$4400.4 - i100.6$	$4393.3 - i101.6$	$4400.9 - i100.5$	
$\frac{5}{2}^+$	$4467.1 - i100.3$	$4457.8 - i140.4$	$4466.7 - i103.2$	
$\frac{5}{2}^+$	$4439.1 - i122.6$	-	$4437.9 - i121.9$	

Extension of JüBo to $\bar{K}N$ scattering: in progress

PhD topic of S. Rawat (FZJ)

- use $SU(3)$ to adapt $\pi N \to X$ model to $\bar{K}N \to X$
- goal: determine hyperon spectrum, i.e. Λ^* and Σ^* states

Selected preliminary fit results $K^- p \to K^0 n$

- Almost finished: coupled-channel fit to $\bar{K}N \to \bar{K}N, \pi\Lambda, \pi\Sigma$
- next step: resonance analysis (pole search)

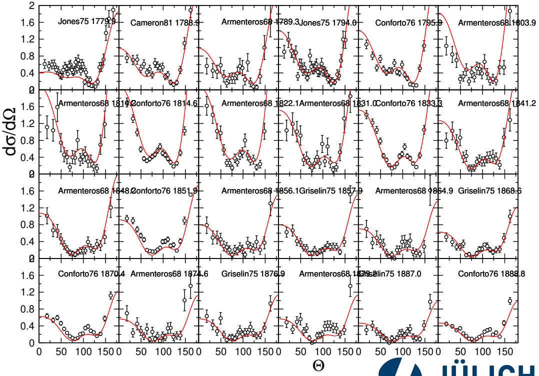

Summary project B.11 ”Coupled-channel dynamics”

Extension of JüBo to

- $K\Lambda$, $K\Sigma$ photoproduction (EPJA 54 (2018) 110, EPJ A 58 (2022) 229, 2404.19404)
- $\pi N \to \omega N$ (Yu-Fei Wang *et al.* PRD 106 (2022))
- hidden-charm channels (Shen CPC 42 (2018), Wang EPJ C 82 (2022), Shen 2405.02626) $\to P_c$ states
- Electroproduction of pions, etas, $K\Lambda$: Jülich-Bonn-Washington collaboration (Mai PRC 103 (2021) 065204, PRC 106 (2022), EPJ A 59 (2023))

Further activities:

- Compositeness or elementariness of baryon resonances (Wang PRC 109 (2024))
- Baryon transition form factors beyond Roper and $\Delta(1232)$, many for the first time (Wang 2404.17444)
- JüBo model for $\bar{K}N$ scattering (hyperon resonance spectrum): PhD project S. Rawat, almost finished
- Coupled channel study of a_0 resonances (Z.-L. Wang, B.-S. Zou EJP C 82 (2022) 509)

Thank you for you attention!

Appendix

Numerical results

Numerical details

Slide by Yu-Fei Wang

- Selection of the resonances
  - JüBo2022 solution ($K\Sigma$ photoproduction, no ωN) [Rönchen *et. al.*, EPJA 58, 229 (2022)]
  - For N^* $J \leq 5/2$, for Δ $J \leq 3/2$
  - Width $\Gamma_R < 300$ MeV
- Uncertainties $\to$ comparison of three results
  - spectral density functions directly from the model
  - locally constructed spectral density functions only by the pole position and residues (L_κ: loop functions)

$$w^{\mathrm{lc}}(z) = -\frac{1}{\pi}\mathrm{Im}\left[z - M_0 - \sum_\kappa g_\kappa^2 L_\kappa(z)\right]^{-1}$$

  - complex compositeness of the Gamow state, with naive measure [Sekihara, PRC 104, 035202 (2021)]

$$\tilde{X}_\kappa \equiv \frac{|X_\kappa|}{\sum_\alpha |X_\alpha| + |Z|}, \tilde{Z} \equiv \frac{|Z|}{\sum_\alpha |X_\alpha| + |Z|}$$

JÜLICH Forschungszentrum

Numerical results

Spectral density functions – Δ states

Blue solid line: the Breit-Wigner denominator. Orange dashed (green dash-dotted) line: the 1st (2nd) spectral density function (model).

Red dotted line: the locally constructed function. Vertical lines: the integral region.

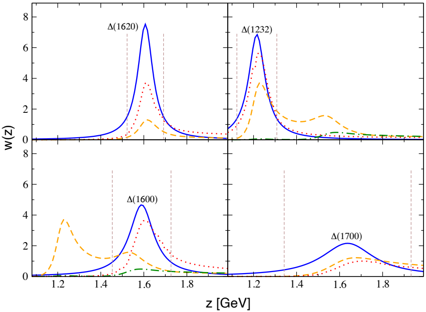

Local construction of the spectral density functions

Slide by Yu-Fei Wang

- Local simulation of the amplitude

$$T^{\rm lc}_{\alpha\beta}(z)=\frac{c g_\alpha g_\beta f^a_\alpha(q_{\alpha z}) f^c_\beta(q_{\beta z})}{z-M_0-\sum_\kappa g_\kappa^2 L_\kappa(z)}+\cdots$$

- Loop functions (f: vertex function in this model)

$$L_\kappa(z)\equiv\int_0^\infty p^2 dp\, G_\kappa(p,z) f^a_\alpha(q_{\kappa z}) f^c_\alpha(q_{\kappa z})$$

- Parameters

$$h_\kappa \equiv \frac{g_\kappa^2}{g_1^2}=\left|\frac{r_\kappa f^a_1}{r_1 f^a_\kappa}\right|^2 ,$$

$$g_1^2=-\frac{\Gamma_R}{2\sum_\kappa h_\kappa \mathrm{Im}(L^{II}_\kappa)} ,$$

$$M_0=M_R-g_1^2\sum_\kappa h_\kappa \mathrm{Re}(L^{II}_\kappa) ,$$

$$c=\frac{r_1^2}{g_1^2 f^a_1 f^c_1}\left(1-g_1^2\sum_\kappa h_\kappa \frac{d}{dz}L^{II}_\kappa\Big|_{z=M_R-i\Gamma_R/2}\right) .$$

- $g^2<0\to$ construction fails. Estimation:

$$g_\kappa^2\to\left|\sqrt{\frac{2\pi\rho_\kappa}{\Gamma_R}}r_\kappa\right|^2 , M_0\to M_0-i\frac{\Gamma_0}{2}$$

Details hidden charm

TABLE I: The new isospin factors used in this work.

Process	Exchanged Particle	$\mathrm{IF}\left(\frac{1}{2}\right)$	$\mathrm{IF}\left(\frac{3}{2}\right)$
$\bar{D}^{(*)}\Lambda_c \to J/\psi N$	D/D^*	1	0
	Λ_c	1	0
$\bar{D}^{(*)}\Sigma_c^{(*)} \to J/\psi N$	D/D^*	$-\sqrt{3}$	0
	Σ_c	$-\sqrt{3}$	0

Photoproduction in a semi-phenomenological approach

EPJ A 50, 101 (2015)

Multipole amplitude

$$M^{IJ}_{\mu\gamma} = V^{IJ}_{\mu\gamma} + \sum_{\kappa} T^{IJ}_{\mu\kappa} G_{\kappa} V^{IJ}_{\kappa\gamma}$$

(partial wave basis)

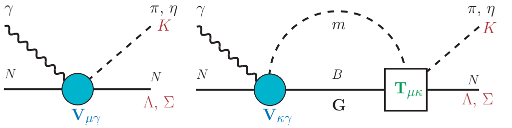

$m = \pi, \eta, K$, $B = N, \Delta, \Lambda$

$T_{\mu\kappa}$: full hadronic T-matrix as in pion-induced reactions

Photoproduction potential: approximated by energy-dependent polynomials (field-theoretical description numerically too expensive)

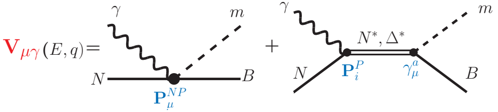

$$= \frac{\tilde{\gamma}^a_\mu(q)}{m_N} P^{\rm NP}_\mu(E) + \sum_i \frac{\gamma^a_{\mu;i}(q) P^{\rm P}_i(E)}{E - m^b_i}$$

JÜLICH Forschungszentrum

Combined analysis of pion- and photon-induced reactions

Data base

Reaction	Observables (# data points)	p./channel
$\pi N \to \pi N$	PWA GW-SAID WI08 [?] (ED solution)	3,760
$\pi^- p \to \eta n$	$d\sigma/d\Omega$ (676), P (79)	755
$\pi^- p \to K^0 \Lambda$	$d\sigma/d\Omega$ (814), P (472), β (72)	1,358
$\pi^- p \to K^0 \Sigma^0$	$d\sigma/d\Omega$ (470), P (120)	590
$\pi^- p \to K^+ \Sigma^-$	$d\sigma/d\Omega$ (150)	150
$\pi^+ p \to K^+ \Sigma^+$	$d\sigma/d\Omega$ (1124), P (551) , β (7)	1,682
$\gamma p \to \pi^0 p$	$d\sigma/d\Omega$ (18721), Σ (3287), P (768), T (1404), $\Delta\sigma_{31}$ (140),	
	G (393), H (225), E (1227), F (397), $C_{x'_L}$ (74), $C_{z'_L}$ (26)	26,662
$\gamma p \to \pi^+ n$	$d\sigma/d\Omega$ (5670), Σ (1456), P (265), T (718), $\Delta\sigma_{31}$ (231),	
	G (86), H (128), E (903)	9,457
$\gamma p \to \eta p$	$d\sigma/d\Omega$ (9112), Σ (535), P (63), T (291), F (144), E (306), G (47), H (56)	10,554
$\gamma p \to K^+ \Lambda$	$d\sigma/d\Omega$ (2563), P (1663), Σ (459), T (383),	
	$C_{x'}$ (121), $C_{z'}$ (123), $O_{x'}$ (66), $O_{z'}$ (66), O_x (314), O_z (314),	6,072
$\gamma p \to K^+ \Sigma^0$	$d\sigma/d\Omega$ (4381), P (422), Σ (280), T (127), $C_{x'}$ (94), $C_{z'}$ (94,) O_x (127), O_z (127)	5,652
$\gamma p \to K^0 \Sigma^+$	$d\sigma/d\Omega$ (281), P (167)	448
	in total	67,008

Selected results $\gamma p \to K^0\Sigma^+$

JüBo2022 **Eur.Phys.J.A 58 (2022) 229**

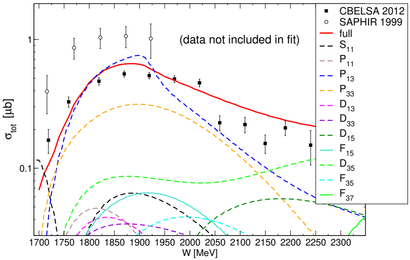

- much less data than for $K^+\Sigma^0$
  (448 vs 5,652 data points)
- in parts inconsistent data
  very few polarization, no double polarization data

  $\to$ difficult to achieve a good fit result
  ($\chi^2 = 3.16$ ($K^0\Sigma^+$) vs 1.66 ($K^+\Sigma^0$))
- cusp in σ_{tot} at $\sim$ 2 GeV not reproduced
  (data not included in fit)

Selected fit results:

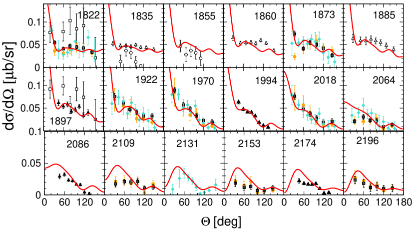

Data: open squares: SPAHIR 1999, cyan: SAPHIR 2005, orange: CBELSA/TAPS 2007, black squares: CBELSA/TAPS 2011, open circles: A2 2018, open triangles: A2 2013, black triangles: Hall B 2003, black circles: CLAS 2013

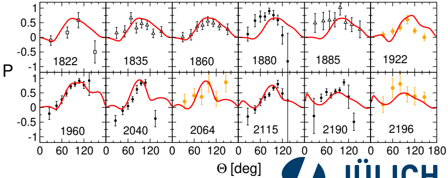

New data for $\gamma p \to K^0\Sigma^+$

L. Clark et al. 2404.19404 [nucl-ex]

Fit JüBo2023-1, together with CLAS Collaboration

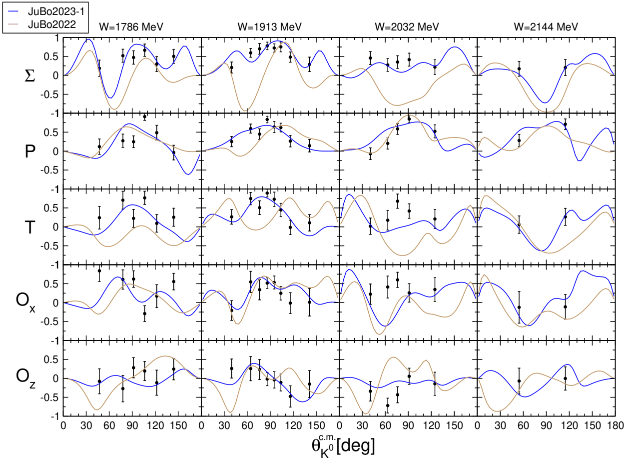

- 105 new data points, first ever for T, O_x, O_z
- simultaneous fit to full JüBo data base including new data
- $\chi^2 = 2.01$ ($K^0\Sigma^+$)

JÜLICH Forschungszentrum

New data for $\gamma p \to K^0\Sigma^+$

L. Clark et al. 2404.19404 [nucl-ex]

Fit JüBo2023-1, together with CLAS Collaboration

Resonance analysis:

$\Delta(1910)\ 1/2^+$	Re E_0	-2Im E_0
2032-1	1745	433
2022	1802 (11)	550 (22)
$N(2190)\ 7/2^-$		
2032-1	1946	162
2022	1965 (12)	288 (66)
$N(1900)\ 3/2^+$		
2032-1	1893	105
2022	1905 (3)	93 (4)

(all numbers in [MeV])

Partial wave content:

- JüBo2022: dominant PW in $K^0\Sigma^+$: P_{13}, followed by P_{33}
- JüBo2023-1: order reversed

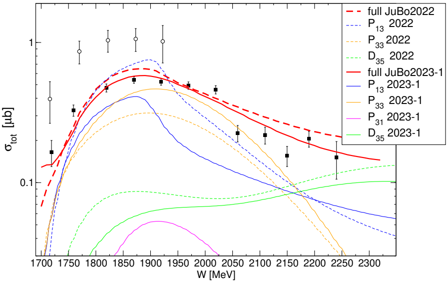

$\Rightarrow$ (Double) polarization data very important to determine the resonance spectrum!

JÜLICH Forschungszentrum

New data for $\gamma p \to K^0\Sigma^+$

L. Clark et al. 2404.19404 [nucl-ex]

Fit JüBo2023-1, together with CLAS Collaboration

Resonance analysis:

$\Delta(1910)$ $1/2^+$	Re E_0	-2Im E_0
2032-1	1745	433
2022	1802 (11)	550 (22)
$N(2190)$ $7/2^-$		
2032-1	1946	162
2022	1965 (12)	288 (66)
$N(1900)$ $3/2^+$		
2032-1	1893	105
2022	1905 (3)	93 (4)

(all numbers in [MeV])

Partial wave content:

- JüBo2022: dominant PW in $K^0\Sigma^+$: P_{13}, followed by P_{33}
- JüBo2023-1: order reversed

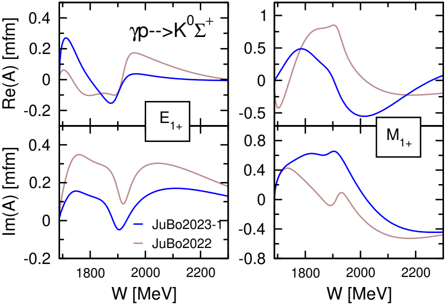

⇒ (Double) polarization data very important to determine the resonance spectrum!

JÜLICH Forschungszentrum

s-, t- and u-channel exchanges

- 21 s-channel states (resonances) coupling to πN, ηN, $K\Lambda$, $K\Sigma$, $\pi\Delta$, ρN.
- t- and u-channel exchanges ("*background*", coupling constants fixed from SU(3)):

	πN	ρN	ηN	πΔ	σN	KΛ	KΣ
πN	N,Δ,$(\pi\pi)_\sigma$, $(\pi\pi)_\rho$	N, Δ, Ct., π, ω, a_1	N, a_0	N, Δ, ρ	N, π	Σ, Σ*, K*	Λ, Σ, Σ*, K*
ρN		N, Δ, Ct., ρ	-	N, π	-	-	-
ηN			N, f_0	-	-	K*, Λ	Σ, Σ*, K*
πΔ				N, Δ, ρ	π	-	-
σN					N, σ	-	-
KΛ						Ξ, Ξ*, f_0, ω, ϕ	Ξ, Ξ*, ρ
KΣ							Ξ, Ξ*, f_0, ω, ϕ, ρ

Excited states / Resonances

$J^P = 3/2^+, I = 3/2$

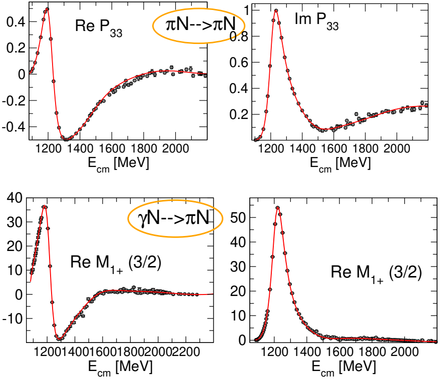

Points: SAID 2006 and CM12

Breit-Wigner parameterization:

$$\mathcal{M}_{ba}^{Res} = -\frac{g_b g_a}{E^2 - M_{BW}^2 + iE\Gamma_{BW}}$$

- M_{BW}, Γ_{BW} channel dependent
- background? overlapping resonances? thresholds?

Excited states / Resonances

$J^P = 1/2^-, I = 3/2$

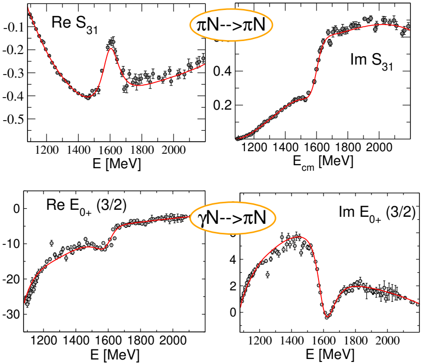

Points: SAID 2006 and CM12

Breit-Wigner parameterization:

$$\mathcal{M}_{ba}^{Res} = -\frac{g_b g_a}{E^2 - M_{BW}^2 + iE\Gamma_{BW}}$$

- M_{BW}, Γ_{BW} channel dependent
- background? overlapping resonances? thresholds?

Excited states / Resonances

$J^P = 1/2^-, I = 3/2$

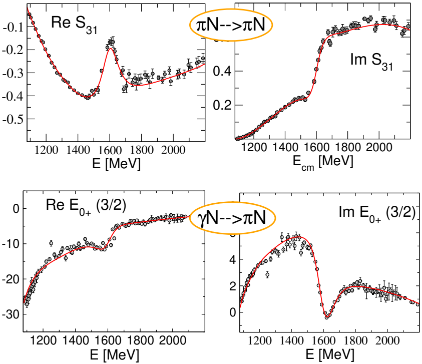

Points: SAID 2006 and CM12

Breit-Wigner parameterization:

$$\mathcal{M}^{Res}_{ba} = -\frac{g_b g_a}{E^2 - M^2_{BW} + iE\Gamma_{BW}}$$

- M_{BW}, Γ_{BW} channel dependent
- background? overlapping resonances? thresholds?

Resonances: poles in the T-matrix on the 2nd Riemann sheet

- Pole position E_0 is the same in all channels
- thresholds: branch points

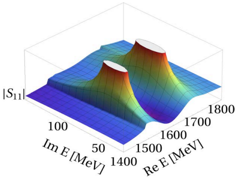

Re(E_0) = "mass"

-2Im(E_0) = "width"

residues$\rightarrow$ branching ratios

Details of the formalism

Polynomials:

$$P_i^{\mathrm{P}}(E) = \sum_{j=1}^{n} g_{i,j}^{\mathrm{P}} \left(\frac{E - E_0}{m_N}\right)^j e^{-g_{i,n+1}^{P}(E-E_0)}$$

$$P_\mu^{\mathrm{NP}}(E) = \sum_{j=0}^{n} g_{\mu,j}^{\mathrm{NP}} \left(\frac{E - E_0}{m_N}\right)^j e^{-g_{\mu,n+1}^{\mathrm{NP}}(E-E_0)}$$

- $E_0 = 1077$ MeV
- $g_{i,j}^{\mathrm{P}}$, $g_{\mu,j}^{\mathrm{NP}}$: fit parameter
- $e^{-g(E-E_0)}$: appropriate high energy behavior
- $n = 3$

back

The scattering potential: s-channel resonances

$$V^{\mathrm{P}} = \sum_{i=0}^{n} \frac{\gamma^a_{\mu;i}\,\gamma^c_{\nu;i}}{z - m^b_i}$$

- i: resonance number per PW
- $\gamma^c_{\nu;i}$ ($\gamma^a_{\mu;i}$): creation (annihilation) vertex function
  with **bare coupling** f (free parameter)
- z: center-of-mass energy
- m^b_i: **bare mass** (free parameter)

- $J \leq 3/2$:

  $\gamma^c_{\nu;i}$ ($\gamma^a_{\mu;i}$) from effective $\mathcal{L}$

Vertex	$\mathcal{L}_{int}$
$N^*(S_{11})N\pi$	$\frac{f}{m_\pi}\bar{\Psi}_{N*}\gamma^\mu\vec{\tau}\,\partial_\mu\vec{\pi}\,\Psi + \text{h.c.}$
$N^*(S_{11})N\eta$	$\frac{f}{m_\pi}\bar{\Psi}_{N*}\gamma^\mu\partial_\mu\eta\,\Psi + \text{h.c.}$
$N^*(S_{11})N\rho$	$f\,\bar{\Psi}_{N*}\gamma^5\gamma^\mu\vec{\tau}\,\vec{\rho}_\mu\,\Psi + \text{h.c.}$
$N^*(S_{11})\Delta\pi$	$\frac{f}{m_\pi}\bar{\Psi}_{N*}\gamma^5\vec{S}\partial_\mu\vec{\pi}\,\Delta^\mu + \text{h.c.}$

- $5/2 \leq J \leq 9/2$:
  correct dependence on L (centrifugal barrier)

$$(\gamma^{a,c})_{\frac{5}{2}-} = \frac{k}{M}(\gamma^{a,c})_{\frac{3}{2}+} \qquad (\gamma^{a,c})_{\frac{5}{2}+} = \frac{k}{M}(\gamma^{a,c})_{\frac{3}{2}-}$$

$$(\gamma^{a,c})_{\frac{7}{2}-} = \frac{k^2}{M^2}(\gamma^{a,c})_{\frac{3}{2}-} \qquad (\gamma^{a,c})_{\frac{7}{2}+} = \frac{k^2}{M^2}(\gamma^{a,c})_{\frac{3}{2}+}$$

$$(\gamma^{a,c})_{\frac{9}{2}-} = \frac{k^3}{M^3}(\gamma^{a,c})_{\frac{3}{2}+} \qquad (\gamma^{a,c})_{\frac{9}{2}+} = \frac{k^3}{M^3}(\gamma^{a,c})_{\frac{3}{2}-}$$

Interaction potential from effective Lagrangian

J. Wess and B. Zumino, Phys. Rev. **163**, 1727 (1967); U.-G. Meißner, Phys. Rept. **161**, 213 (1988); B. Borasoy and U.-G. Meißner, Int. J. Mod. Phys. A **11**, 5183 (1996).

- consistent with the approximate (broken) chiral $SU(2) \times SU(2)$ symmetry of QCD

Vertex	$\mathcal{L}_{int}$	Vertex	$\mathcal{L}_{int}$
$NN\pi$	$-\frac{g_{NN\pi}}{m_\pi}\Psi\gamma^5\gamma^\mu\vec{\tau}\cdot\partial_\mu\vec{\pi}\Psi$	$NN\omega$	$-g_{NN\omega}\bar{\Psi}[\gamma^\mu - \frac{\kappa_\omega}{2m_N}\sigma^{\mu\nu}\partial_\nu]\omega_\mu\Psi$
$N\Delta\pi$	$\frac{g_{N\Delta\pi}}{m_\pi}\bar{\Delta}^\mu\vec{S}^\dagger\cdot\partial_\mu\vec{\pi}\Psi$ + h.c.	$\omega\pi\rho$	$\frac{g_{\omega\pi\rho}}{m_\omega}\epsilon_{\alpha\beta\mu\nu}\partial^\alpha\vec{\rho}^\beta\cdot\partial^\mu\vec{\pi}\omega^\nu$
$\rho\pi\pi$	$-g_{\rho\pi\pi}(\vec{\pi}\times\partial_\mu\vec{\pi})\cdot\vec{\rho}^\mu$	$N\Delta\rho$	$-i\frac{g_{N\Delta\rho}}{m_\rho}\bar{\Delta}^\mu\gamma^5\gamma^\mu\vec{S}^\dagger\cdot\vec{\rho}_{\mu\nu}\Psi$ + h.c.
$NN\rho$	$-g_{NN\rho}\Psi[\gamma^\mu - \frac{\kappa_\rho}{2m_N}\sigma^{\mu\nu}\partial_\nu]\vec{\tau}\cdot\vec{\rho}_\mu\Psi$	$\rho\rho\rho$	$g_{NN\rho}(\vec{\rho}_\mu\times\vec{\rho}_\nu)\cdot\vec{\rho}^{\mu\nu}$
$NN\sigma$	$-g_{NN\sigma}\bar{\Psi}\Psi\sigma$	$NN\rho\rho$	$\frac{\kappa_\rho g^2_{NN\rho}}{2m_N}\bar{\Psi}\sigma^{\mu\nu}\vec{\tau}\Psi(\vec{\rho}_\mu\times\vec{\rho}_\nu)$
$\sigma\pi\pi$	$\frac{g_{\sigma\pi\pi}}{2m_\pi}\partial_\mu\vec{\pi}\cdot\partial^\mu\vec{\pi}\sigma$	$\Delta\Delta\pi$	$\frac{g_{\Delta\Delta\pi}}{m_\pi}\bar{\Delta}_\mu\gamma^5\gamma^\nu\vec{T}\Delta^\mu\partial_\nu\vec{\pi}$
$\sigma\sigma\sigma$	$-g_{\sigma\sigma\sigma}m_\sigma\sigma\sigma\sigma$	$\Delta\Delta\rho$	$-g_{\Delta\Delta\rho}\bar{\Delta}_\tau(\gamma^\mu - i\frac{\kappa_{\Delta\Delta\rho}}{2m_\Delta}\sigma^{\mu\nu}\partial_\nu)$ $\cdot\vec{\rho}_\mu\cdot\vec{T}\Delta^\tau$
$NN\rho\pi$	$\frac{g_{NN\pi}}{m_\pi}2g_{NN\rho}\bar{\Psi}\gamma^5\gamma^\mu\vec{\tau}\Psi(\vec{\rho}_\mu\times\vec{\pi})$	$NN\eta$	$-\frac{g_{NN\eta}}{m_\pi}\bar{\Psi}\gamma^5\gamma^\mu\partial_\mu\eta\Psi$
NNa_1	$-\frac{g_{NN\pi}}{m_\pi}m_{a_1}\bar{\Psi}\gamma^5\gamma^\mu\vec{\tau}\Psi\vec{a}_\mu$	NNa_0	$g_{NNa_0}m_\pi\bar{\Psi}\vec{\tau}\Psi\vec{a}_0$
$a_1\pi\rho$	$-\frac{2g_{\pi a_1\rho}}{m_{a_1}}[\partial_\mu\vec{\pi}\times\vec{a}_\nu - \partial_\nu\vec{\pi}\times\vec{a}_\mu]\cdot[\partial^\mu\vec{\rho}^\nu - \partial^\nu\vec{\rho}^\mu]$ $+\frac{2g_{\pi a_1\rho}}{2m_{a_1}}[\vec{\pi}\times(\partial_\mu\vec{\rho}_\nu - \partial_\nu\vec{\rho}_\mu)]\cdot[\partial^\mu\vec{a}^\nu - \partial^\nu\vec{a}^\mu]$	$\pi\eta a_0$	$g_{\pi\eta a_0}m_\pi\eta\vec{\pi}\cdot\vec{a}_0$

Generalization to SU(3)

to include KY final states

- t- and u-channel exchange: T^{NP}

  coupling constants fixed from SU(3) symmetry

  e.g. $g_{\Lambda NK} = -\frac{\sqrt{3}}{3} g_{NN\pi} (1 + 2\alpha_{BBP})$

  J. J. de Swart, Rev. Mod. Phys. **35**, 916 (1963) [Erratum-ibid. **37**, 326 (1965)].

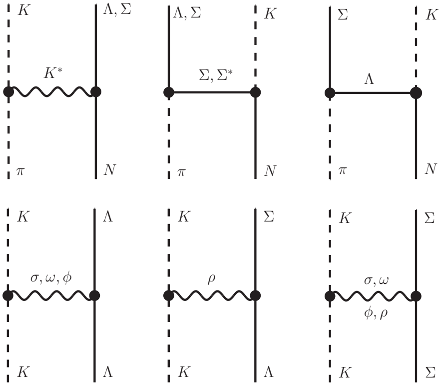

New free parameters: cutoffs Λ

- s-channel: resonances

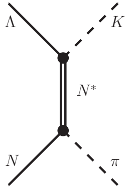

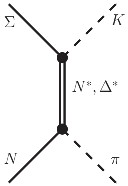

New free parameters:
bare couplings g_{N^*KY} and $g_{\Delta^* K\Sigma}$

Theoretical constraints of the S-matrix

Unitarity: probability conservation

- 2-body unitarity
- 3-body unitarity:

  discontinuities from t-channel exchanges

  $\rightarrow$ Meson exchange from requirements of the S-matrix [Aaron, Almado, Young, Phys. Rev. 174, 2022 (1968)]

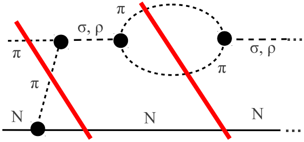

Analyticity: from unitarity and causality

- correct structure of branch point, right-hand cut (real, dispersive parts)
- to approximate left-hand cut $\rightarrow$ Baryon u-channel exchange

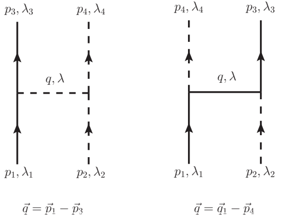

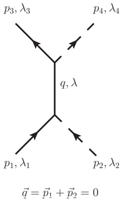

$\rightarrow$ Resonances

Λ decay parameter α_-

Advantage in KY photoproduction: self-analysing decay of the hyperons
$\rightarrow$ measurement of recoil polarization easier

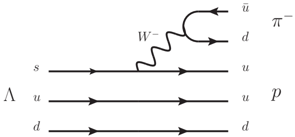

- Λ decays weakly to $\pi^- p$ with decay parameter α_- (PDG average: $\alpha_- = 0.642 \pm 0.013$)
- recent BESIII measurement ($e^+e^- \rightarrow J/\psi \rightarrow \Lambda\bar{\Lambda}$):
  $\alpha_- = 0.750 \pm 0.009 \pm 0.004$ (Ablikim, Nature (2019))

  $\rightarrow$ polarizations affected by α_- are $\sim$ 17% too large!
- independent estimation of α_- from $\gamma p \rightarrow K^+\Lambda$ CLAS data using Fierz identities
  $\Rightarrow \alpha_- = 0.721 \pm 0.006 \pm 0.005$ (Ireland et al. PRL 123 (2019))

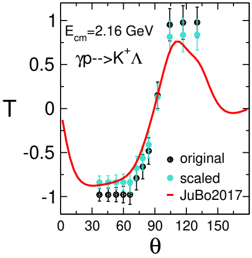

data: Paterson (CLAS) PRC 93, 065201 (2016)

Has impact on

- observables P, T, C_x, C_z, O_x, O_z
- reactions $\gamma p \rightarrow K^+\Lambda$, $K^+\Sigma^0$ ($\rightarrow K^+\gamma\Lambda$), $\pi^- p \rightarrow K^0\Lambda$, $K^0\Sigma^0$
- resonance spectrum? $\Rightarrow$ **JüBo re-fit to data scaled by new α_-**

JÜLICH Forschungszentrum